Sperm gatekeeping: 3D imaging reveals a constricted entrance to zebra finch sperm storage tubules

Authors: Tania Mendonca[1,2], Ashley J Cadby[2] and Nicola Hemmings[1]

[1]Department of Animal and Plant Sciences, University of Sheffield, Western Bank, Sheffield S10 2TN, UK

[2]Department of Physics and Astronomy, University of Sheffield, Western Bank, Sheffield S10 2TN, UK

Corresponding author: Tania Mendonca (t.mendonca@sheffield.ac.uk)

Short Title: Visualising female sperm storage

Abstract:

Females across many internally fertilising taxa store sperm, often in specialised storage organs in their reproductive tracts. In birds, several hundred sperm storage tubules exist in the utero-vaginal junction of the oviduct and there is growing evidence that sperm storage in these tubules is selective. The nature of the mechanisms underlying female sperm storage in birds remains unknown due to our limited ability to make three dimensional, live observations inside the large, muscular avian oviduct. Here, we describe a new application of fluorescence selective plane illumination microscopy to optically section oviduct tissue from zebra finch *Taeniopygia guttata* females label-free, by harnessing tissue autofluorescence. Our data provide the first description of the 3D structure of sperm storage tubules in any bird, and reveal the presence of constricted openings to tubules, suggesting active entrapment and release of sperm.

26 **Introduction:**

27 Across many internal fertilisers, females have evolved the capacity to maintain viable
28 sperm in specialised sperm storage organs in their reproductive tract as a strategy to
29 maximise fertility. Sperm storage ensures the female has sufficient sperm for fertilisation
30 when copulation and ovulation are not synchronised [1]. Since female promiscuity is
31 common across taxa (e.g. birds [2], mammals [3–5], reptiles [6], fishes [7] and insects [8–
32 10]), storage also provides the opportunity for females to exert control over post-
33 copulatory processes [11–13]. Post-copulatory sexual selection has driven the
34 diversification of sperm storage organs, which vary from single bean-shaped structures
35 in many damselfly species [14,15], to one or more sac-like spermathecae in certain fly
36 species (e.g. three spermathecae in *Scathophaga stercoraria* [16]; two spermathecae
37 along with a seminal receptacle in many Drosophila species [17]), and multiple epithelial
38 crypts in snakes [18], lizards [19], turtles [20] and birds [21,22].

39

40 In birds, epithelial sperm storage crypts are called sperm storage tubules (SSTs) and are
41 located in the utero-vaginal junction (UVJ) of the oviduct [23]. The number of SSTs
42 possessed by a single female ranges from around 500 SSTs in the UVJ of the budgerigar
43 *Melopsittam undulatus* to 20,000 in the turkey *Meleagris gallopavo* [24]. A growing body
44 of evidence suggests that avian SSTs may be an important site of sperm selection. Steele
45 and Wishart [25] demonstrated experimentally that when chicken sperm were treated to
46 remove surface proteins from their membranes, they could not enter the SSTs after
47 normal intra-vaginal artificial insemination, even though sperm treated in the same way
48 were capable of fertilising the ovum when inseminated further up the oviduct, past the
49 vagina and UVJ. Bobr *et al.* [23] also noted a lack of abnormal sperm in the SSTs of
50 domestic fowl *Gallus domesticus*, suggesting that abnormal sperm are unable to reach or

enter sperm storage sites. The large number of SSTs present in the avian oviduct may also allow spatio-temporal segregation of sperm from competing ejaculates within the oviduct [26–28]. However, the mechanisms by which sperm are selected at the time of storage remain poorly understood, and how sperm enter and exit the SSTs is unknown.

The role of the SSTs in sperm storage and selection may be relatively passive. Froman [29] proposed a model where sperm motility, rather than SST function, is pivotal in sperm retention in SSTs. According to this model, sperm must maintain an optimum swimming velocity to maintain their position and counter a fluid current within the SST. This model was supported by evidence that faster sperm emerged out of SSTs later than slower sperm [30], and that passive loss of sperm from storage might be sufficient to explain last male precedence in the domestic fowl, turkeys, and zebra finches *Taeniopygia guttata* [31,32; but see 27]. However, there have been no observations of sperm swimming inside the SSTs, and other studies have detected the presence of sperm motility suppressors such as lactic acid in Japanese quail *Coturnix japonica* SSTs [33], calcium and zinc in the SSTs of chicken, turkeys and Japanese quail [34,35], and carbonic anhydrase in the SSTs of turkeys, common quail *Coturnix coturnix* and ostriches *Struthio camelus* [36–38]. The neurotransmitter acetylcholine, released by nerve endings detected in the vicinity of SSTs [39], has been shown to enhance sperm motility [40], implying a nervous control on sperm mobilisation at ejection from SSTs. Additionally, Hiyama *et al.* [41] presented evidence for the potential role of heat shock protein 70 (HSP70) [42] in enhancing sperm motility at the point of sperm release. HSP70 proteins were found to be localised on the surface epithelium of the UVJ and their levels were upregulated ~20h post oviposition in Japanese quail, coincidental with when sperm have been shown to be released from storage in these birds [41]. The presence of such sperm motility suppressors and

activators within or near the SSTs suggests storage may not be as passive as Froman [29] suggested.

It is possible that rather than acting as passive refugia, SSTs may be dynamic structures, capable of active constriction and dilation to mediate the entrance and exit of sperm. Although numerous studies have failed to find smooth muscle fibres or myoepithelial cells [39,43,44] around SSTs, Freedman *et al.* [39] detected fibroblast-like cells and an F-actin rich cytoskeletal mesh called the "terminal web" in turkey SST epithelia. The terminal web is composed of contractile proteins (actin and myosin) and has been shown to contribute to contractility in other tissues, such as intestinal brush border cells [45,46] and embryonic pigmented epithelia in chicken [47]. Freedman *et al.* [39] also found terminal innervations in the turkey UVJ, suggesting there may be some degree of nervous control over SST function. Recent evidence also suggests the possibility of SST contraction, influenced hormonally by the action of progesterone [48,49]. It is therefore possible that the passage of sperm into and out of storage is controlled, to some degree, by the physical structure of SSTs themselves.

Our understanding of how SST structure influences sperm storage is limited by our relatively basic knowledge of SST morphology. The avian oviduct is convoluted, with opaque, muscular walls, creating numerous practical limitations for making observations of tubules in living epithelial tissue using conventional microscopy techniques. Empirical studies of SST morphology have so far used histology [23,50,51] and electron microscopy [34,43,52] on fixed tissue sections, but these approaches not only remove functional information, but typically provide two-dimensional information only. Moreover, serial sectioning is laborious, and loss of material can be difficult to avoid. Commonly used light

101 microscopy techniques rely on thin sections and squash preparations [26,53], which are
102 largely inappropriate for large tissue samples since they distort structures of interest and
103 allow only limited imaging depths.
104
105 In this study we used selective plane illumination microscopy (SPIM), to develop a novel
106 method for live, *ex vivo* imaging and examining the 3D structure of avian SSTs for the first
107 time. SPIM has been demonstrated to be highly suitable for imaging large samples at
108 cellular resolution with lower phototoxicity levels than with other optical sectioning
109 methods [54,55]. Using SPIM, we were able to optically section tissue up to depths of 100
110 μm, so that entire folds of UVJ mucosal tissue could be imaged live without distorting or
111 damaging their structure. We provide the first true estimates of the 3D structure of avian
112 SSTs in living tissue, including the relationship between SST length and diameter, and
113 report the existence of a previously unreported physical constriction at the entrance to
114 tubules that may act to regulate sperm transport into and out of storage. We also find no
115 evidence of sperm motility inside or on release from sperm storage tubules, providing
116 support for the idea that sperm motility is suppressed inside the SSTs.
117

118 **Materials and Methods:**

119

120 *Animals*

121 Zebra finches were from a captive population kept at the University of Sheffield
122 [56,57]. Females (all between one to three years old) were placed in unisex housing
123 for at least two weeks before being paired with males, in cages (dimensions of each:
124 0.6m x 0.5m x 0.4m) placed side-by-side and separated by a wire-mesh with the male
125 and female on either side. A modified nest-box with a wire-mesh partition was

126 supplied to each pair. This set up ensured that the male and female established a
127 normal breeding pair bond, leading the female to come into breeding condition, while
128 ensuring that she had no sperm in her SSTs (sperm can be stored for up to 12 days
129 after mating in zebra finches [24]). Only females from this no-copulation set-up were
130 used for SST structural imaging, and all imaging methods described below, unless
131 stated otherwise, refer to this part of the study. For a separate study, a small number
132 of females were allowed to copulate with males, and from these females we collected
133 data on sperm motility inside and on release from the SSTs using different methods
134 (see "Sperm motility" below). Females were only used once they had started to lay
135 eggs, to ensure their oviduct was in full reproductive condition. After the second egg
136 in the ovulatory cycle, females were euthanized (in accordance with Schedule 1
137 [Animals (Scientific Procedures) Act 1986)] and dissected immediately.
138
139 *Sample preparation*
140 The oviduct, including the cloaca, was immediately removed from the female and the
141 connective tissue surrounding it was cleared to uncoil and straighten the vagina and
142 the UVJ. The lower end of the oviduct was cut through the middle of the uterus to
143 obtain a segment that included the UVJ, vagina and cloaca. This piece of the oviduct
144 was then cut open lengthwise and pinned flat on a petri-dish filled with silicone
145 elastomer (SYLGARD® 184; Dow Corning). A sufficient quantity of Ham's F10 Nutrient
146 Mix (Invitrogen, UK) was added to keep the tissue moist but not submerged. For SPIM
147 imaging, UVJ folds were cut individually with iris scissors and mounted one at a time,
148 on a custom-made sample holder (supplementary materials) using fine insect needles.
149 The sample holder, with the UVJ fold mounted, was immersed in phenol-free
150 DMEM/F12 media, at 37º C during imaging.

151

152 *SPIM imaging*

153 Live UVJ tissue samples, prepared as above, were imaged using a custom-built SPIM
154 microscope (at the University of Sheffield) with laser excitation at 473 nm and a 520
155 nm long pass (LP) fluorescence emission filter (Semrock, Inc.). The microscope
156 hardware and optical components are based on the OpenSPIM platform [58] but with
157 modifications detailed in Mendonca *et al*. [59 supplementary materials]. The camera,
158 detection and illumination objectives, and magnification are fixed for the system,
159 ensuring that the imaging results are reproduceable. The autofluorescence image
160 stacks were acquired using 500 ms exposure, starting at the outer surface and moving
161 up to 100 μm deep into the tissue fold.

162

163 *Characterisation of autofluorescence*

164 SSTs were clearly identifiable in live UVJ tissue during fluorescence imaging on the
165 SPIM and had a punctate appearance on account of autofluorescent granules (Figure
166 1, (B and D)) which appeared to be mostly confined to SST epithelial cells and were
167 present along the entire length of the SST from orifice to blind end. No other cell
168 structure or organelle was visible in these autofluorescence images.

169

170 To determine the organisation of the autofluorescent granules in the SST epithelium,
171 label-free images from live UVJ folds (n = 10 birds) were acquired on the SPIM were
172 compared to those of fixed UVJ tissue folds, imaged on the SPIM after staining for
173 nucleic acids (n = 3 birds), and on a bright-field microscope after histological
174 sectioning and general histochemical staining (n = 3 birds) (Supplementary
175 materials).

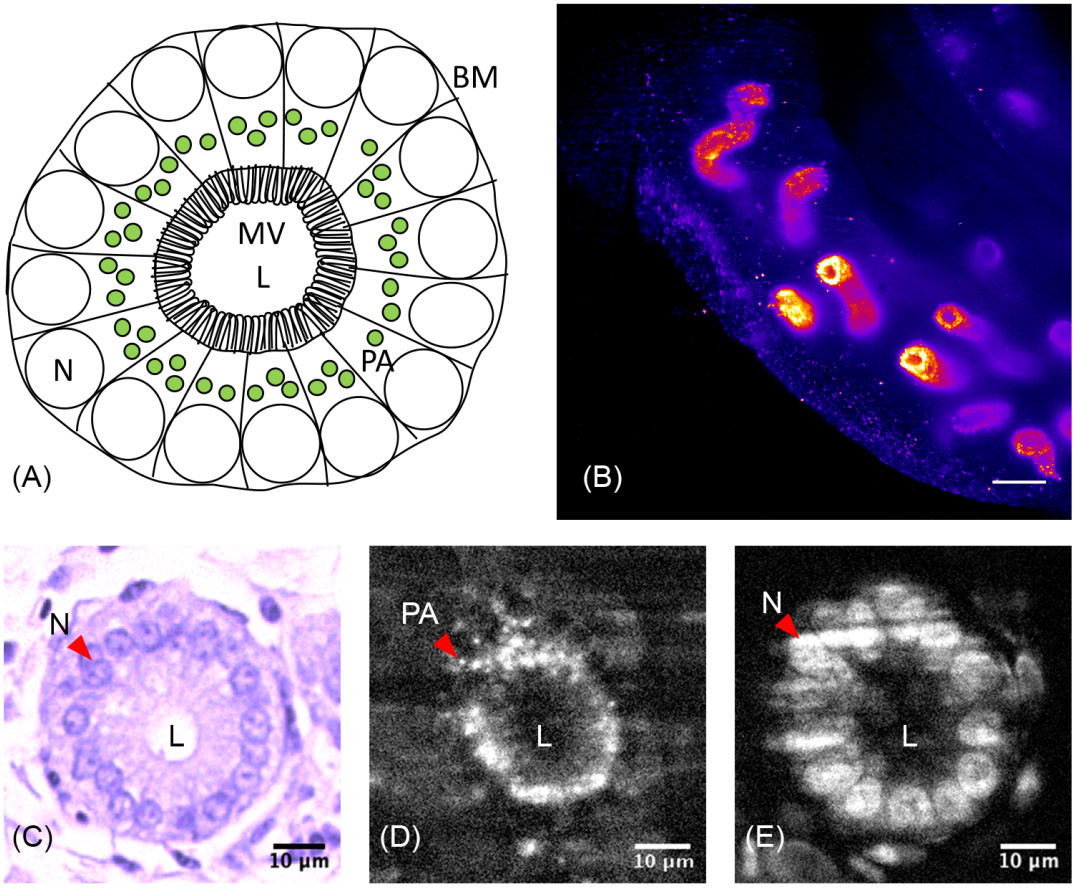

Figure 1: (A) Schematic of SST transverse section showing cellular polarisation with nuclei (N) towards the basement membrane (BM) and microvilli (MV) at the apical end of the epithelium. The punctate autofluorescence (PA) detected by the SPIM is present proximal to the nucleus but not at the apical end of the epithelium near the lumen (L). (B) Max intensity projection of a UVJ fold with multiple detectable SSTs imaged on the SPIM. (C)-(E) Cross section of SST from histology, autofluorescence imaged on the SPIM, and SYTO-13 labelled nuclei imaged on the SPIM respectively.

Image Analysis

The image stacks acquired using the SPIM were used to reconstruct 480 µm x 480 µm x 100 µm tissue sections containing 3D information on SST structure (n = 10 females, one SST per female). SST shape information was extracted by measuring the diameter

enclosed by the autofluorescence from images of live tissue, at ten equidistant points along the length of the SST.

UVJ tissue image stacks were first pre-processed in Fiji [60]. Individual unbranched SSTs were selected from each female such that the entire SST structure was included in the 3D image stacks. The SSTs follow convoluted paths through the UVJ fold tissue, so in order to measure cross-sectional diameter at multiple points, it was necessary to slice the image volume at arbitrary angles to ensure the measurement planes were perpendicular to the direction of the SST structure. This was accomplished by first tracing the direction of the SST structure using a dilated version of the SST image (generated using the 'MorphoLibJ' plugin [61] followed by the application of Gaussian blur), to smooth the punctate autofluorescence. Two outlines for each SST were then semi-automatically traced in 3D, from the orifice to the blind end and along opposite sides of the SST lumen, using the 'Simple Neurite Tracer' [62] plugin in Fiji.

The next stage of image analysis was performed using MATLAB® (2015b, version 8.6, MathWorks, Natick, MA). An average trace which passed through the SST lumen was computed from the two traces for each SST. SST lengths were measured from these average traces. For each SST (n = 10), the average trace was interpolated at ten equidistant points (the first at the orifice and the tenth point before the blind end of the tubule) and at each interpolated point a vector describing the direction of the SST at that point was computed using its nearest neighbouring points on the trace. By using these vectors and the interpolated points, slicing planes normal to the vectors were defined. The indices for these slicing planes were used to extract 2D image sections from the un-dilated original image stacks using the 'ExtractSlice.m' [63]

215 function. For every extracted slice, its distance from the orifice along the luminal trace
216 of the SST was computed using the 'Arclength.m' [64] function, and the major axis
217 diameter (d1) and the minor axis diameter (d2) of the SST (enclosed by
218 autofluorecence) were measured.
219
220 *Sperm motility*
221 To test the hypothesis that sperm are motile in the SSTs [29], we used tissue from a
222 subset of 13 females from a separate study, that had copulated with males prior to
223 dissection (and therefore had sperm inside their SSTs). These females were dissected
224 as described above, but instead of mounting UVJ folds for SPIM imaging, folds were
225 dissected on a microscope slide under a Nikon SMZ25 stereomicroscope to isolate and
226 open individual SSTs and release sperm. We identified one SST per fold (46 SSTs in
227 total) with high numbers of stored sperm (mean = 33 per SST), isolated the SST using
228 methods described in [28] and submerged it in warmed nutrient media (Ham's F10:
229 Invitrogen, UK; typically used for avian sperm motility analysis) on a microscope slide.
230 The slide was then placed on a heated stage (set at 38º C) and observed under a 200X
231 phase contrast microscope for 5 mins to screen for sperm motility inside the tubule. After
232 this initial observation period, the SST was pulled open to release sperm using fine
233 dissection needles, as described in [28], and sperm were gently shaken free of the tubule.
234 The slide was then observed under a 200X phase contrast microscope for another 5 mins
235 to screen for sperm motility after release from the tubule.
236
237 **Statistical Analysis:**
238 Data analysis was performed using the statistical package R, version 3.2.3 [65]. We
239 tested whether SST diameter varied with SST length using a mixed effects model

240 ('lmer' function from the 'lme4' package [66] along with the 'lmerTest' package [67])
241 with average SST diameter [(d1+ d2) / 2] at the sampled point as the dependent
242 variable, the distance of sampled point from SST orifice and the SST total length as
243 fixed effects, and the bird ID as a random effect to account for repeated measures from
244 each female.
245
246 We also assessed if the SST was elliptical or circular in cross-section (the former
247 providing greater epithelial apical surface area for increased contact with sperm) and
248 whether any such ellipticity changed in response to SST length. A circularity index was
249 first calculated by dividing the major axis diameter (d1) by the minor axis diameter
250 (d2), where a circularity index of one indicates a circular SST cross-section. Data were
251 then analysed via a mixed effects model using the 'lmer' function [66], with the
252 circularity index as the dependent variable and the total length of the SST as a fixed
253 effect. The sum of the major and minor axis diameters (d1+ d2) was also incorporated
254 as a fixed effect to account for magnitude of change in diameter along each axis, as
255 well as the distance of sampled point from SST orifice, with an interaction term
256 between them. As before, bird ID was included as a random effect to account for
257 repeated measures from each female.
258
259 **Results:**
260 The diameter of SSTs was found to be notably constricted at their orifice, suggestive
261 of a structural 'barrier' for entry and exit (Figure 2 (A)). SST diameter increased
262 slightly increase along the SST's length up to a mid-point, after which it decreased
263 slightly towards the blind end of the SST, resulting in a significant quadratic
264 relationship between SST diameter and the distance from the SST orifice (estimated

effect = -16.761, t = -3.085, p = 0.003; Figure 2 (B)). There was no relationship between SST length and either mean, maximum, or minimum diameter, so long SSTs were neither wider nor thinner than short SSTs (estimated effect = 0.038, t = 1.058, p = 0.319; Figure 4). The relationship between SST diameter and distance from orifice also held true with data from labelled tissue (Supplementary Figure S4), confirming that the shape measured from autofluorescence images was real and not an artefact resulting from the distribution of the autofluorescence granules.

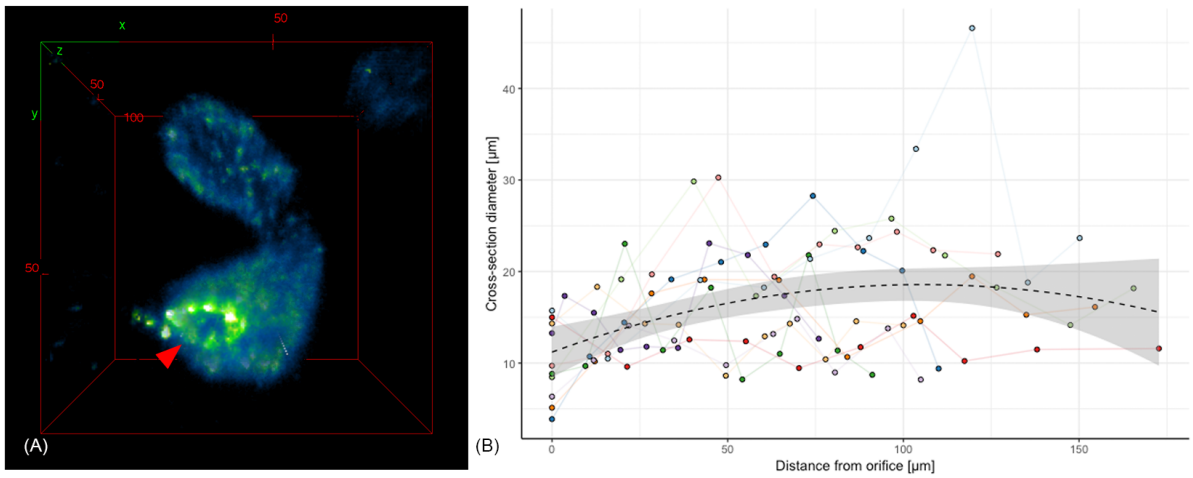

Figure 2: (A) 3D rendering of an SST showing its constricted orifice (arrowhead). (B) SST diameter has a quadratic relationship with distance from the SST opening suggesting a constriction at the orifice and a slight increase in diameter along its length up to the middle of the SST. Each colour on the plot represents measurements from the same SST (n = 10). Scale on red bounding box is in microns.

SSTs were found to be slightly elliptical in cross-section, with the major axis diameter being 1.642 ± 0.168 times larger than the minor axis diameter. The circularity of the SST in cross-section did not vary significantly with SST diameter (estimated effect = 0.014, t = 0.979, p = 0.330), distance from orifice (estimated effect = 0.003, t = 0.587, p = 0.558), or the interaction between these two variables (estimated effect = -

285 0.00009, t = -0.587, p = 0.559). Circularity was also not related to SST total length
286 (estimated effect = -0.004, t = -1.14, p = 0.282).
287
288 Comparisons between the SST measurements from histology and SPIM images
289 indicate that the autofluorescent granules are present in the supranuclear region of
290 the SST epithelium (Figure 1). The size of the lumen diameter scaled linearly with the
291 width of the SST (Supplementary Figure S4), indicating that epithelial cells remained
292 the same thickness in cross-section with increasing SST diameter. This allowed us to
293 extrapolate shape information from the above analyses to the SST lumen, and using
294 this method, we estimated the diameter of the SST orifice to be 3.278 ± 1.115 μm
295 (mean ± SD; Table 1).
296
297 Finally, we found no evidence of sperm motility either inside, or on release from, the
298 SSTs. Of 1520 sperm across 46 SSTs (from 13 females), no sperm were observed
299 actively swimming before or after release from the tubules.
300
301 **Table 1: SST dimensions at orifice and widest section**

	Diameter (mean ± SD)	
	at orifice (μm)	**at widest section (μm)**
inter-nuclear diameter[1]	12.060 ± 1.419	30.830 ± 11.055
autofluorescence[1]	10.065 ± 4.288	16.374 ± 6.610
lumen diameter[2]	3.278 ± 1.115	9.128 ± 1.377

302 SST diameter is the smallest at its orifice and widest at the relative slice position 'slice 6', where
303 slice 1 is at the orifice and slice 10 is nearest to the blind end of the SST.
304 [1]Measurements acquired from SPIM image z-stacks
305 [2]SST lumen diameter values were predicted from the model describing the relationship between
306 lumen and inter-nuclear diameter.

307

308 **Discussion:**

309 Using novel 3D imaging methods, we have demonstrated for the first time the
310 existence of a constricted orifice at the entrance/exit of avian SSTs. Although the
311 precise function of this constriction remains to be identified, it is likely that it plays
312 an important role in sperm selection and storage. Consistent with previous findings
313 of an F-actin rich terminal web in the SSTs in turkeys [39], this constricted opening is
314 suggestive of contractile activity for active entrapment and release of sperm.
315 However, even without contractility, the narrow SST orifice (mean diameter of about
316 3 μm), with the added obstruction of microvilli (1-2 μm in length, [52]) could restrict
317 the rate of sperm (mean diameter at mid-piece - ~0.6 μm [59]) entering and exiting
318 the SST, thereby providing a mechanism by which sperm storage and release can be
319 regulated. This, combined with the fact that sperm do not appear to actively swim
320 inside or on immediate release from the tubules, supports the idea that avian SSTs
321 play an active and selective role in sperm storage, regulating sperm uptake and
322 release and suppressing motility [33–38]. The constricted orifice, together with its
323 microvilli, may act as a valve, allowing unidirectional movement of sperm only, and
324 preventing them from being flushed back out. The small luminal diameter along the
325 SST (mean: 9 μm, Table 1) may also limit the ability of sperm to turn around inside
326 the SST and swim out.

327

328 SSTs were also found to be slightly elliptical in cross-section, with the major axis
329 diameter being about 1.6 times larger than the minor axis diameter. This ellipticity
330 was independent of SST radius, the distance along the SST from orifice, or total SST
331 length. Cross-sectional ellipticity increases the surface area of the SST epithelial apical

332 surface, allowing for a greater number of microvilli (as compared to a circular lumen
333 with the same volume) for increased contact with sperm and optimum exchange of
334 nutrients and waste.
335
336 SST diameter varied widely across SSTs. Birkhead *et al.* [68] suggested that some SSTs
337 might remain inactive in the zebra finch UVJ even in its fully developed state. It is
338 possible that some of the variation in SST shape that we observed can be explained by
339 the presence of functional and non-functional SSTs, but it is unclear whether thinner,
340 more uniform SSTs, or more distended morphs would represent active SSTs. Mero and
341 Ogasawara [69], and Burke [70] described 'swollen' tubules in chicken and suggested
342 swelling to be associated with sperm release. Such swellings might help explain the
343 outliers in our data (Figure 2). It is possible that conformational changes in SST shape
344 from functional to non-functional may be caused by neural stimulation [39,71] and/or
345 hormonal effects [48,49], potentially aiding sperm release. Variation in SST shape
346 might also be explained by factors not tested in this study, including age, hormone
347 levels and location of the SST in the UVJ.
348

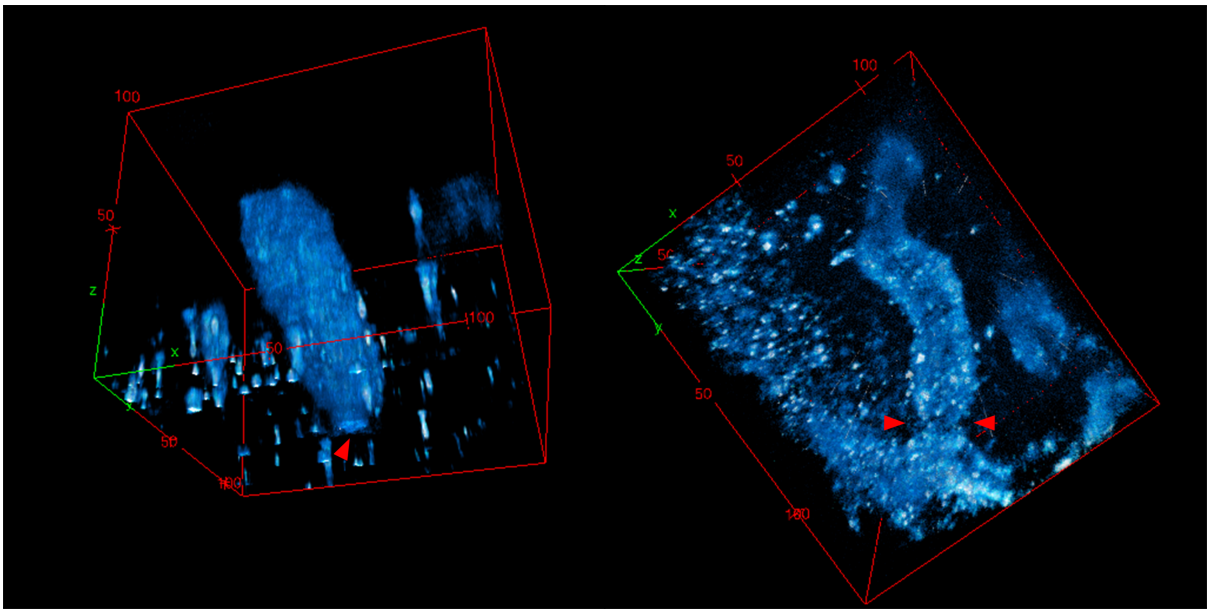

Figure 3: Sperm storage tubules (SSTs) imaged label-free using the SPIM. SST shape showed a constricted opening (arrowheads) but varied between more elliptical shapes (left) and thinner, more uniform shapes (right). Scale on red bounding box is in microns.

About 4 – 27% of all the sperm storage tubules in the zebra finch UVJ are branched [28,72]. These were not included in the present study, but individual branches are expected to show similar shapes as unbranched tubules. Hemmings and Birkhead [28] described sperm from different males differentially stored in separate branches of a branched SST (albeit a single observation, since in most cases sperm from different males were stored in different SSTs). Further study of the 3D structure of branched SSTs could shed light on the mechanisms that might prevent sperm mixing in branched tubules.

Our novel 3D data on SST structure was made possible by the presence of punctate/granular autofluorescence, confined to the SST epithelial cells and uniformly distributed throughout the SST's entire length. These granules were found to have a supranuclear localisation in the SST epithelial cells (Figure 1). Although

367 identifying the exact source of the autofluorescence was beyond the scope of this
368 study, autofluorescence in a similar range has been noted in the ewe *Ovis aries*
369 endometrium ($\lambda_{ex}/\lambda_{em}$ = 488/525-575 nm) [73] and in human colonic crypts ($\lambda_{ex}/\lambda_{em}$
370 = 488/580 nm) [74]. While such autofluorescence has been attributed to NADH
371 metabolism in mitochondria [73,75], another likely source might be lipofuscin in
372 lysosomes [74]. Mitochondria are not confined to the apical cytoplasm of SST
373 epithelium as observed in turkeys [76] and domestic fowl [77] so it is unlikely that
374 these granules represent mitochondria. Lysosomes on the other hand, are globular
375 vesicles similar to the autofluorescent granules observed here in size (< 1 μm) [78],
376 and have been detected in the apical cytoplasm of turkey SST epithelia [76], and less
377 abundantly in domestic fowl [77] and passerine alpine accentor *Prunella collaris* [78].
378 Multiple studies have also detected the presence of acid phosphatase, an enzyme
379 found in lysosomes, in the supranuclear cytoplasm of SST epithelia in turkeys [21],
380 quail [79], domestic fowl [80] and ducks *Anas sp.* [81], but not in the SST lumen, which
381 corresponds with the autofluorescence pattern we observed here. Acid phosphatase
382 has been implicated in autolysis associated with oviduct regression [82] as well as
383 with sperm release [81]. If this is true, the label-free imaging methods developed here
384 may provide exciting new means for investigating SST functional development
385 throughout the reproductive cycle. Identifying the chemical nature of the
386 autofluorescent substance present in SST granules therefore represents an important
387 avenue for future research.
388
389 In summary, we have demonstrated that SSTs in living avian oviductal tissue can be
390 imaged label-free using SPIM microscopy, and this novel 3D imaging technique has
391 enabled us to produce the most detailed account of avian SST structure to date,

including the discovery of a previously unknown structural constriction at the entrance/exit of tubules that may play a key role in the regulation of sperm storage and selection. The imaging methods described here hold immense potential for studying SST function and interactions with sperm in real time.

Ethics:

This study was approved by the University of Sheffield, UK. All procedures performed conform to the legal requirements for animal research in the UK and were conducted under a project licence (PPL 40/3481) issued by the Home Office. Animals were humanely killed under Schedule 1 (Animals (Scientific Procedures) Act 1986).

Competing interests:

The authors declare no conflict of interest.

Authors' contributions:

T.M. coordinated the study, conducted the experiments and analyses, and wrote the manuscript; N.H. conceived the study and advised on data analyses. All authors participated in the design of the study, helped draft the manuscript and gave final approval for publication.

Acknowledgements:

The authors are grateful to Prof Tim Birkhead and Prof Simon Jones from the University of Sheffield for support. Thanks to Mark Kinch from Skelet.AL, Phil Young, Lynsey Gregory, Emily Glendenning and Jamie Thompson from the University of Sheffield for technical assistance.

Funding:

TM was funded by an Imagine: Imaging Life studentship granted by the University of Sheffield. NH was funded by ERC grant no. 268688 and a Patrick and Irwin-Packington Independent Research Fellowship from the Department of Animal & Plant Sciences, University of Sheffield.

420 **References**:

421 1. Birkhead TR. 1992 Sperm Storage and the Fertile Period in the Bengalese Finch.
422 *Auk* **109**, 620–625. (doi:10.2307/4088376)
423 2. Birkhead TR, Møller AP. 1995 Extra-pair copulation and extra-pair paternity in
424 birds. *Anim. Behav.* **49**, 843–848. (doi:10.1016/0003-3472(95)80217-7)
425 3. Hanken J, Sherman PW. 1981 Multiple paternity in Belding's ground squirrel
426 litters. *Science (80-.).* **212**, 351–353. (doi:10.1126/science.7209536)
427 4. Tegelström H, Searle J, Brookfield J, Mercer S. 1991 Multiple paternity in wild
428 common shrews (Sorex araneus) is confirmed by DNA-fingerprinting. *Heredity*
429 *(Edinb).* **66 (Pt 3)**, 373–379. (doi:10.1038/hdy.1991.47)
430 5. Amos W, Twiss S, Pomeroy PP, Anderson SS. 1993 Male mating success and
431 paternity in the grey seal, Halichoerus grypus: a study using DNA fingerprinting.
432 *Proc. R. Soc. B* **252**, 199–207. (doi:10.1098/rspb.1993.0066)
433 6. Uller T, Olsson M. 2008 Multiple paternity in reptiles: Patterns and processes.
434 *Mol. Ecol.* **17**, 2566–2580. (doi:10.1111/j.1365-294X.2008.03772.x)
435 7. Avise JC, Jones AG, Walker D, DeWoody JA. 2002 Genetic mating systems and
436 reproductive natural histories of fishes: lessons for ecology and evolution. *Annu.*
437 *Rev. Genet.* **36**, 19–45. (doi:10.1146/annurev.genet.36.030602.090831)
438 8. Gromko MH, Gilbert DG, Richmond RC. 1984 Sperm transfer and use in the
439 multiple mating system of Drosophila. *Sperm Compet. Evol. Anim. mating Syst.* ,
440 371–426.
441 9. Moritz RFA, Kryger P, Koeniger G, Koeniger N, Estoup A, Tingek S. 1995 High
442 degree of polyandry in Apis dorsata queens detected by DNA microsatellite
443 variability. *Behav. Ecol. Sociobiol.* **37**, 357–363. (doi:10.1007/BF00174141)
444 10. Crozier RH, Fjerdingstad EJ. 2001 Polyandry in social Hymenoptera - disunity in

445 diversity? *Ann. Zool. Fennici* **38**, 267–285. (doi:10.2307/23735845)

446 11. Birkhead TR, Møller AP. 1998 *Sperm competition and sexual selection*. Academic
447 Press.

448 12. Simmons LW. 2001 *Sperm competition and its evolutionary consequences in the*
449 *insects*. Princeton University Press.

450 13. Eberhard WG. 1996 *Female Control: Sexual Selection by Cryptic Female Choice*.
451 Princeton University Press.

452 14. Córdoba-Aguilar A, Uhía E, Rivera AC. 2003 Sperm competition in Odonata
453 (Insecta): the evolution of female sperm storage and rivals' sperm displacement. *J.*
454 *Zool.* **261**, 381–398. (doi:10.1017/S0952836903004357)

455 15. Siva-Jothy MT. 1987 The structure and function of the female sperm-storage
456 organs in libellulid dragonflins. *J. Insect Physiol.* **33**, 559–567. (doi:10.1016/0022-
457 1910(87)90070-9)

458 16. Ward PI. 1993 Females influence sperm storage and use in the yellow dung fly
459 Scathophaga stercoraria (L.). *Behav. Ecol. Sociobiol.* **32**.
460 (doi:10.1007/BF00183786)

461 17. Pitnick S, Markow T, Spicer GS. 1999 Evolution of Multiple Kinds of Female
462 Sperm-Storage Organs in Drosophila. *Evolution (N. Y).* **53**, 1804.
463 (doi:10.2307/2640442)

464 18. Fox W. 1956 Seminal receptacles of snakes. *Anat. Rec.* **124**, 519–539.
465 (doi:10.1002/ar.1091240303)

466 19. Conner J, Crews D. 1980 Sperm transfer and storage in the lizard Anolis
467 carolinensis. *J. Morphol.* **163**, 331–348.

468 20. Gist DH, Jones JM. 1989 Sperm storage within the oviduct of turtles. *J. Morphol.*
469 **199**, 379–384. (doi:10.1002/jmor.1051990311)

470 21. Zavaleta D, Ogasawara F. 1973 A review of the mechanism of the release of
471 spermatozoa from storage tubules in the fowl and turkey oviduct. *Worlds. Poult.*
472 *Sci. J.* **43**, 132–139. (doi:10.1079/WPS19870010)
473 22. Bakst MR. 1987 Anatomical basis of sperm-storage in the avian oviduct. *Scanning*
474 *Microsc.* **1**, 1257.
475 23. Bobr LW, Lorenz FW, Ogasawara FX. 1964 Distribution of Spermatozoa in the
476 Oviduct and Fertility in Domestic Birds. I. Residence Sites of Spermatozoa in Fowl
477 Oviducts. *J. Reprod. Fertil.* **8**, 39–47. (doi:10.1530/JRF.0.0110257)
478 24. Birkhead TR, Møller AP. 1992 Numbers and size of sperm storage tubules and the
479 duration of sperm storage in birds: a comparative study. *Biol. J. Linn. Soc.* **45**, 363–
480 372. (doi:10.1111/j.1095-8312.1992.tb00649.x)
481 25. Steele MG, Wishart GJ. 1996 Demonstration that the removal of sialic acid from
482 the surface of chicken spermatozoa impedes their transvaginal migration.
483 *Theriogenology* **46**, 1037–1044. (doi:http://dx.doi.org/10.1016/S0093-
484 691X(96)00268-3)
485 26. King LM, Brillard JP, Garrett WM, Bakst MR, Donoghue AM. 2002 Segregation of
486 spermatozoa within sperm storage tubules of fowl and turkey hens. *Reproduction*
487 **123**, 79–86. (doi:10.1530/rep.0.1230079)
488 27. Briskie J V. 1996 Spatiotemporal patterns of sperm storage and last-male sperm
489 precedence in birds. *Funct. Ecol.* **10**, 375–383. (doi:10.2307/2390286)
490 28. Hemmings N, Birkhead TR. 2017 Differential sperm storage by female zebra
491 finches Taeniopygia guttata. *Proc. R. Soc. B* **284**, 20171032.
492 (doi:10.1098/rspb.2017.1032)
493 29. Froman DP. 2003 Deduction of a model for sperm storage in the oviduct of the
494 domestic fowl (Gallus domesticus). *Biol. Reprod.* **69**, 248–53.

495 (doi:10.1095/biolreprod.102.013482)
496 30. Froman DP, Pizzari T, Feltmann AJ, Castillo-Juarez H, Birkhead TR. 2002 Sperm
497 mobility: mechanisms of fertilizing efficiency, genetic variation and phenotypic
498 relationship with male status in the domestic fowl, Gallus gallus domesticus. *Proc.*
499 *R. Soc. B* **269**, 607–12. (doi:10.1098/rspb.2001.1925)
500 31. Birkhead TR, Pellatt JE, Hunter FM. 1988 Extra-pair copulation and sperm
501 competition in the zebra finch. *Nature* **334**, 60–2. (doi:10.1038/334060a0)
502 32. Birkhead TR, Biggins JD. 1998 Sperm competition mechanisms in birds: models
503 and data. *Behav. Ecol.* **9**, 253–260. (doi:10.1093/beheco/9.3.253)
504 33. Matsuzaki M *et al.* 2015 Lactic acid is a sperm motility inactivation factor in the
505 sperm storage tubules. *Sci. Rep.* **5**, 17643. (doi:10.1038/srep17643)
506 34. Holm L, Ekwall H, Wishart GJ, Ridderstråle Y, Ridderstrale Y. 2000 Localization of
507 calcium and zinc in the sperm storage tubules of chicken, quail and turkey using
508 X-ray microanalysis. *J. Reprod. Fertil.* **118**, 331–336.
509 (doi:10.1530/reprod/118.2.331)
510 35. Bakst MR, Richards MP. 1985 Concentrations of selected cations in turkey serum
511 and oviductal mucosae. *Poult. Sci.* **64**, 555–563.
512 36. Holm L, Ridderstråle Y. 1998 Localization of carbonic anhydrase in the sperm-
513 storing regions of the turkey and quail oviduct. *Histochem. J.* **30**, 481–488.
514 (doi:10.1023/A:1003247504288)
515 37. Holm L, Wishart GJ. 1998 The effect of pH on the motility of spermatozoa from
516 chicken, turkey and quail. *Anim. Reprod. Sci.* **54**, 45–54. (doi:10.1016/S0378-
517 4320(98)00142-0)
518 38. Holm L, Ruziwa SD, Dantzer V, Ridderstråle Y. 2000 Carbonic anhydrase in the
519 utero-vaginal junction of immature and mature ostriches. *Br. Poult. Sci.* **41**, 244–9.

520 (doi:10.1080/713654906)
521 39. Freedman SL, Akuffo VG, Bakst MR. 2001 Evidence for the innervation of sperm
522 storage tubules in the oviduct of the turkey (Meleagris gallopavo). *Reproduction*
523 **121**, 809–814. (doi:10.1530/reprod/121.5.809)
524 40. Atherton RW, Cisson CM, Wilson BW, Golder TK. 1980 Quantitation of avian
525 spermatozoan motility: Neurochemical regulation. *Gamete Res.* **3**, 17–24.
526 (doi:10.1002/mrd.1120030104)
527 41. Hiyama G, Matsuzaki M, Mizushima S, Dohra H, Ikegami K, Yoshimura T, Shiba K,
528 Inaba K, Sasanami T. 2014 Sperm activation by heat shock protein 70 supports
529 the migration of sperm released from sperm storage tubules in Japanese quail
530 (Coturnix japonica). *Reproduction* **147**, 167–178. (doi:10.1530/rep-13-0439)
531 42. Lindquist S, Craig EA. 1988 the Heat -Shock Proteins. *Annu. Rev. Genet.* **22**, 631–
532 677. (doi:https://doi.org/10.1146/annurev.ge.22.120188.003215)
533 43. Van Krey HP, Ogasawara FX, Pangborn J. 1967 Light and Electron Microscopic
534 Studies of Possible Sperm Gland Emptying Mechanisms. *Poult. Sci.* **46**, 69–78.
535 (doi:10.3382/ps.0460069)
536 44. Gilbert AB, Reynolds ME, Lorenz FW. 1968 Distribution of spermatozoa in the
537 oviduct and fertility in domestic birds. V. Histochemistry of the uterovaginal
538 sperm-host glands of the domestic hen. *J. Reprod. Fertil.* **16**, 433–44.
539 (doi:10.1530/jrf.0.0160433)
540 45. Hirokawa N, Keller TCS, Chasan R, Mooseker MS. 1983 Mechanism of brush
541 border contractility studied by the quick-freeze, deep-etch method. *J. Cell Biol.* **96**,
542 1325–1336. (doi:10.1083/jcb.96.5.1325)
543 46. Keller TCS, Conzelman KA, Chasan R, Mooseker MS. 1985 Role of myosin in
544 terminal web contraction in isolated intestinal epithelial brush borders. *J. Cell*

545 *Biol.* **100**, 1647–1655. (doi:10.1083/jcb.100.5.1647)
546 47. Owaribe K, Kodama R, Eguchi G. 1981 Demonstration of contractility of
547 circumferential actin bundles and its morphogenetic significance in pigmented
548 epithelium in vitro and in vivo. *J. Cell Biol.* **90**, 507–514.
549 (doi:10.1083/jcb.90.2.507)
550 48. Ito T, Yoshizaki N, Tokumoto T, Ono H, Yoshimura T, Tsukada A, Kansaku N,
551 Sasanami T. 2011 Progesterone is a sperm-releasing factor from the sperm-
552 storage tubules in birds. *Endocrinology* **152**, 3952–3962. (doi:10.1210/en.2011-
553 0237)
554 49. Hemmings N, Birkhead TR, Brillard JP, Froment P, Briere S. 2015 Timing
555 associated with oviductal sperm storage and release after artificial insemination
556 in domestic hens. *Theriogenology* **83**, 1174–1178.
557 (doi:10.1016/j.theriogenology.2014.12.022)
558 50. Bakst MR. 1998 Structure of the avian oviduct with emphasis on sperm storage in
559 poultry. *J. Exp. Zool.* **282**, 618–626. (doi:10.1002/(SICI)1097-
560 010X(199811/12)282:4/5<618::AID-JEZ11>3.0.CO;2-M)
561 51. Van Drimmelen GC. 1946 'Spermnests' in the oviduct of the domestic hen. *J. South*
562 *African Vet. Med. Assoc* **17**, 42–52.
563 52. Bakst MR, Bauchan G. 2015 Apical blebs on sperm storage tubule epithelial cell
564 microvilli: Their release and interaction with resident sperm in the turkey hen
565 oviduct. *Theriogenology* **83**, 1438–44.
566 (doi:10.1016/j.theriogenology.2015.01.016)
567 53. Bakst MR. 1992 Observations on the turkey oviductal sperm-storage tubule using
568 differential interference contrast microscopy. *J. Reprod. Fertil.* **95**, 877–883.
569 54. Huisken J, Swoger J, Del Bene F, Wittbrodt J, Stelzer EHK. 2004 Optical Sectioning

570 Deep Inside Live Embryos by Selective Plane Illumination Microscopy. *Science*
571 *(80-.).* **305**, 1007–1009. (doi:10.1126/science.1100035)
572 55. Reynaud EG, Krzic U, Greger K, Stelzer EHK. 2008 Light sheet-based fluorescence
573 microscopy: more dimensions, more photons, and less photodamage. *HFSP J.* **2**,
574 266–75. (doi:10.2976/1.2974980)
575 56. Birkhead TR, Pellatt JE, Brekke P, Yeates R, Castillo-Juarez H. 2005 Genetic effects
576 on sperm design in the zebra finch. *Nature* **434**, 383–7.
577 (doi:10.1038/nature03374)
578 57. Bennison C, Hemmings N, Slate J, Birkhead T. 2015 Long sperm fertilize more
579 eggs in a bird. *Proc. R. Soc. B* **282**, 20141897. (doi:10.1098/rspb.2014.1897)
580 58. Pitrone PG, Schindelin J, Stuyvenberg L, Preibisch S, Weber M, Eliceiri KW,
581 Huisken J, Tomancak P. 2013 OpenSPIM: an open-access light-sheet microscopy
582 platform. *Nat. Methods* **10**, 598–599. (doi:10.1038/nmeth.2507)
583 59. Mendonca T, Birkhead TR, Cadby AJ, Forstmeier W, Hemmings N. 2018 A trade-
584 off between thickness and length in the zebra finch sperm mid-piece. *Proc. R. Soc.*
585 *B Biol. Sci.* **285**, 20180865. (doi:10.1098/rspb.2018.0865)
586 60. Schindelin J *et al.* 2012 Fiji: an open-source platform for biological-image analysis.
587 *Nat. Methods* **9**, 676–82. (doi:10.1038/nmeth.2019)
588 61. Legland D, Arganda-Carreras I, Andrey P. 2016 MorphoLibJ: integrated library
589 and plugins for mathematical morphology with ImageJ. *Bioinformatics* **32**, 3532–
590 3534. (doi:10.1093/bioinformatics/btw413)
591 62. Longair MH, Baker DA, Armstrong JD. 2011 Simple neurite tracer: Open source
592 software for reconstruction, visualization and analysis of neuronal processes.
593 *Bioinformatics* **27**, 2453–2454. (doi:10.1093/bioinformatics/btr390)
594 63. Teng P. 2011 Extract Slice from Volume.

595 64. D'Errico J. 2012 arclength.
596 65. R Development Core Team. 2015 *R: A Language and Environment for Statistical*
597 *Computing*. R Foundation for Statistical Computing, Vienna, Austria. See
598 https://www.r-project.org/.
599 66. Bates DM, Machler M, Bolker BM, Walker SC. 2014 Fitting Linear Mixed-Effects
600 Models using lme4. *J. Stat. Softw.* **67**, 1--48. (doi:10.18637/jss.v067.i01)
601 67. Kuznetsova A, Brockhoff PB, Christensen RHB. 2017 lmerTest Package: Tests in
602 Linear Mixed Effects Models. *J. Stat. Softw.* **82**, 1–26. (doi:10.18637/jss.v082.i13)
603 68. Birkhead TR, Pellatt JE, Hunter FM. 1990 Numbers and Distribution of Sperm in
604 the Uterovaginal Sperm Storage Tubules of the Zebra Finch. *Condor* **92**, 508–516.
605 (doi:10.2307/1368249)
606 69. Mero KN, Ogasawara FX. 1970 Dimensions of uterovaginal sperm-storage tubules
607 of the chicken and their possible significance in sperm release. *Poult. Sci.* **49**,
608 1304–1308. (doi:10.3382/ps.0491304)
609 70. Burke WH. 1968 Release of spermatozoa from storage sites in the hen's oviduct.
610 Univ. of California, Davis.
611 71. Gilbert AB, Lake PE. 1963 Terminal Innervation of the Uterus and Vagina of the
612 Domestic Hen. *Reproduction* **5**, 41–NP. (doi:10.1530/jrf.0.0050041)
613 72. Birkhead TR, Hunter FM. 1990 Numbers of sperm-storage tubules in the Zebra
614 Finch (Poephila guttata) and Bengalese Finch (Lonchura striata). *Auk* **107**, 193–
615 197.
616 73. Druart X *et al.* 2009 In vivo imaging of in situ motility of fresh and liquid stored
617 ram spermatozoa in the ewe genital tract. *Reproduction* **138**, 45–53. (doi:Doi
618 10.1530/Rfp-09-0108)
619 74. DaCosta RS. 2005 Autofluorescence characterisation of isolated whole crypts and

620 primary cultured human epithelial cells from normal, hyperplastic, and
621 adenomatous colonic mucosa. *J. Clin. Pathol.* **58**, 766–774.
622 (doi:10.1136/jcp.2004.023804)
623 75. Brookner CK, Follen M, Boiko I, Galvan J, Thomsen S, Malpica A, Suzuki S, Lotan R,
624 Richards-Kortum R. 2000 Autofluorescence Patterns in Short-term Cultures of
625 Normal Cervical Tissue. *Photochem. Photobiol.* **71**, 730–736. (doi:10.1562/0031-
626 8655(2000)071<0730:apistc>2.0.co;2)
627 76. Schuppin GT, Van Krey HP, Denbow DM, Bakst MR, Meyer GB. 1984
628 Ultrastructural analyses of uterovaginal sperm storage glands in fertile and
629 infertile turkey breeder hens. *Poult Sci* **63**, 1872–1882.
630 (doi:10.3382/ps.0631872)
631 77. Burke WH, Ogasawara FX, Fuqua CL. 1972 A study of the ultrastructure of the
632 uterovaginal sperm-storage glands of the hen, Gallus domesticus, in relation to a
633 mechanism for the release of spermatozoa. *J. Reprod. Fertil.* **29**, 29–36.
634 (doi:10.1530/jrf.0.0290029)
635 78. Chiba A, Nakamura M. 2001 Microscopic structure of the sperm storage tubules in
636 the polygynandrous alpine accentor, Prunella collaris (Aves). *Acta Zool.* **82**, 299–
637 306. (doi:10.1046/j.1463-6395.2001.00091.x)
638 79. Renden JA, May EB, Benoff FH. 1981 Histochemistry of uterovaginal sperm-host
639 glands in Japanese Quail (Coturnix coturnix japonica) with reference to the period
640 of oviposition. *Poult. Sci.* **60**, 2529–2535. (doi:10.3382/ps.0602529)
641 80. Gilbert AB, Reynolds ME, Lorenz FW. 1968 Distribution of spermatozoa in the
642 oviduct and fertility in domestic birds. 8. The effect of a foreign object in the
643 uterus on secretions of the sperm-host glands and the survival of spermatozoa in
644 the oviduct of the domestic hen. *J. Reprod. Fertil.* **17**, 311–4.

645 (doi:10.1530/jrf.0.0160433)

646 81. Pal D. 1977 Histochemistry of the utero-vaginal junction with special reference to
647 the sperm-host glands in the oviduct of the domestic duck. *Folia Histochem.*
648 *Cytochem. (Krakow).* **15**, 235–42.

649 82. Heryanto B, Yoshimura Y, Tamura T, Okamoto T. 1997 Involvement of Apoptosis
650 and Lysosomal Hydrolase Activity in the Oviducal Regression During Induced
651 Molting in Chickens : A Cytochemical Study for End Labeling of Fragmented DNA
652 and Acid Phosphatase Treatment of Birds and Collection of Samples. *Poult. Sci.* **76**,
653 67–72. (doi:10.1093/ps/76.1.67)

654